Energy Equip. Sys./ Vol. 10/No. 4/Dec. 2022/ 417-437

ENERGY EQUIPSYS

Energy Equipment and Systems

http://energyequipsys.ut.ac.ir
www.energyequipsys.com

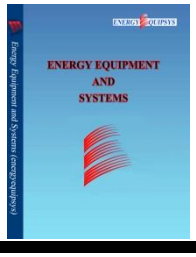

Energy, exergy and environmental analyses of a trigeneration system with power generation units of solid oxide fuel cell and solar panels

Authors

Ali Zahmatkesh[a]
Mahmood Mehregan[a*]

[a] Faculty of Mechanical Engineering, Shahrood University of Technology, Shahrood, Iran, P.O.B. 3619995161

Article history:

Received : 19 March 2022
Accepted : 26 June 2022

ABSTRACT

In this research, a new trigeneration system with the prime mover of solid oxide fuel cells and solar energy was simulated to supply the required energy of a sample building in Shahrood, Iran. For this purpose, at first, the required loads of the building have been calculated. Then, the trigeneration system was used to provide the required heating, cooling, and electrical loads for the building. The analysis was performed for each component of the system from energy aspects. Then the obtained equations were solved using EES software. The results showed that the total amount of electrical power produced by the system in spring and summer is about 1184.5 kW and in autumn and winter is 1121.7 kW. The total electrical energy produced by the system during the year is about 9921112 kWh. Also, 1301.2 MWh of thermal energy was collected by 50 solar panels throughout the year. The electrical efficiency of the fuel cell is 46.77% and the whole system is 53.97%. Also, the thermal efficiency of the whole system is equal to 86.9%. The carbon dioxide emission coefficient is 358.2, which is very low and desirable compared to fossil fuel systems. Due to the intensity of solar radiation in the city of Shahrood, the designed system can provide heat and cold loads for the building well and the efficiency of the trigeneration system is much higher than similar systems and the amount of pollution is much lower.

Keywords: Trigeneration, Solid Oxide Fuel Cell, Solar Energy, Energy Analysis, Environmental Analysis.

1. Introduction

The energy crisis is one of the issues of concern in today's societies. Fossil fuels, which have so far provided much of the energy needed by humans, are a declining resource that will help develop human society in the future [1]. On the other hand, the systems which consume these fuels have low efficiency. Considering the issues of fossil fuel reduction, global warming and the low efficiency of current energy conversion technologies, the use of efficient and modern energy production systems is of paramount importance. Combined generation systems are one of the most important pieces of equipment for increasing energy efficiency [2]. Conventional and old fuel consumption systems, in addition to wasting fuel resources due to low thermal efficiency, are also sources

* Corresponding author: Mahmood Mehregan
Faculty of Mechanical Engineering, Shahrood University of Technology, Shahrood, Iran, P.O.B. 3619995161
Email: mehregan@shahroodut.ac.ir

of environmental pollution. In addition, the extent of pollution from fossil fuels has made life on Earth difficult. Given the above, choosing the right, cheap and clean fuel as an alternative to fossil fuels is necessary. In addition to fuel replacement, the use of new energy conversion systems with high efficiency and low pollution is one of the important and significant solutions in this field [3]. The use of new energy and energy conversion systems with high efficiency and low pollution is necessary. Fuel cells are one of the energy conversion systems. Fuel cell due to their high efficiency and lack of environmental pollution is now a good solution to overcome the energy bottleneck and environmental pollution. The combined heating, cooling and power system is also one of the modern technologies and one of the new energy conversion systems and due to its high efficiency, it is considered by governments and research centers. Therefore, it is necessary to study these types of systems in order to optimize and commercialize them and add new technologies to them, which will be examined in this research [4,5].

These systems can use a variety of prime movers, including gas turbines [1], steam turbines [4-6], internal combustion engines [7-9], Stirling engines [10-14], fuel cells [15-18], and renewable sources [19-21]. Recently, power plants based on fuel cells have received more attention due to their high heat efficiency, low operating costs and low emissions. Systems based on gas turbines [2, 3] and internal combustion engines [8] had good thermal performance, but the emission rate of greenhouse gases and nitrogen oxide compounds in them was very high. Because in these systems, combustion occurs at high temperatures and as a result, various compounds of nitrous oxide (NOx) are formed. These systems are economically justified when they have large-scale production. Also, in systems with steam turbine prime mover [4, 5], the overall performance of the system was lower due to the low thermal efficiency of the system. Furthermore, the start-up time of steam turbines and their initial investment costs are very high [6], so they are not very suitable for use in the combined generation system, especially on a small scale. Stirling engines have good thermal properties because different heat sources can be used in this system, but the most important drawback of these systems is the existence of multiple heat exchangers. The thermal efficiency of these systems is highly dependent on the thermal performance of the converters. Since access to high-performance heat exchangers requires initial costs as well as high maintenance costs, most of these systems are not economically viable.

The aim of this study is to analyze the energy, exergy, and environmental performance of a new Trigeneration system using solar energy and solid oxide fuel cells and to show the potential of using this system for a typical residential building in Shahrood. The sub-objectives of the research are to calculate the effect of current density on voltage and fuel cell power density, electrical efficiency, and the number of solar cells; and to calculate the effect of radiation intensity on energy efficiency and total exergy efficiency.

Nomenclature

A	Area
C	Thermal Capacity
D	Hydraulic diameter
E_{OCV}	Voltage open circuit energy
f	friction coefficient
F	Visibility coefficient
J	Current Density
h	Enthalpy
L	length of the pipe
m	Mass
$\dot{Q}$	Heat flux
T	Temperature
U	Overall heat transfer coefficient
V_{cell}	Cell voltage
$\dot{W}$l	Power

Abbreviations

CHP	combined heat and power
CCHP	combined cooling heat and power
EES	Engineering equation solver
LHV	Lower heating Value
SOFC	Solid oxide fuel cell

Subtitles

c	Collector
$\dot{I}$	Exergy destruction rate
P	Pressure

r	receiver
ele	Electric
$\dot{E}x$l	Exergy
E	Evaporator
SP	Coils inside receiver tubes

Greek symbols

σ	Boltzmann Constant
η	efficiency
ψ	Atomic ratio of hydrogen to carbon
ε	Absorption coefficient
ρ	Density
ΔG_fl	Gibbs free energy
ΔV_{ohm}	Ohmic voltage losses
ΔV_{act}	Activation voltage Losses
ΔV_{trans}l	Transient state voltage losses

2. Literature review

Many different studies have been conducted on combined generation systems with various types of prime movers.

In general, the efficiency of energy conversion systems has technical-economic limitations. Selecting high-efficiency energy conversion technologies, combining energy conversion technologies and using them in CHP systems are suitable solutions to increase the efficiency of the energy conversion system and reduce the unit cost of energy due to technical-economic constraints. In the meantime, solar energy has received much attention due to its being accessible and available. Solar energy can be more economical than other renewable energies, especially in countries with a higher rate of solar irradiance. On the other hand, the fuel cell has high reliability and it is necessary to use it along with solar energy, which is not always available. Therefore, in this study, the main focus has been on solar energy and fuel cells.

Sheykhi et al. [8] investigated the efficiency of a combined heat and power (CHP) system using internal and external combustion engines. They showed that the system's performance is strongly dependent on the rotational speed of the engine and, therefore to provide the load of buildings that do not have a baseload and the consumption pattern has many fluctuations using these systems. Therefore, the system will work for a long time with less efficiency than the nominal value. Chahartaghi et al. [13] developed a thermodynamic model of a combined cooling heating and power (CCHP) system on a beta-type Stirling engine used to reduce fuel consumption and emissions. Their system consists of two beta-Stirling engines as the prime mover, a heat recovery system. , an absorption chiller, and a power generator. The effects of engine speed and heater wall temperature on efficiency, fuel consumption, and emitted carbon dioxide were studied and fuel consumption and carbon dioxide emissions decreased compared to conventional systems.

Chahartaghi et al. [14] investigated the CCHP system consisting of a Stirling engine with helium and hydrogen gases, which could also be used for domestic applications. The non-ideal adiabatic engine was considered and two beta Stirling engines and an absorption chiller were introduced, which work with the heat loss of the engine and the effects of heater speed and temperature, and type of operating gases on the coefficient of performance and CCHP efficiency, reduce operating costs. The reduction of dioxide emissions compared to conventional methods was investigated and the results were shown for both gases separately.

Calise et al. [22] investigated the design and dynamic simulation of a cogeneration system using photovoltaic thermal (PVT) collectors. In their research, they designed and simulated a system for generating heat and cold and electrical energy using solar energy. The temperature provided by the solar collector was about 80 degrees Celsius. For this reason, a one-stage absorption chiller of lithium bromide was used to provide refrigeration in the system. The system was designed to provide power, heat, hot water and cooling to a university building in Italy. Finally, this system was analyzed from an energy and economic perspective. They used TRNSYS software to simulate the system.

Buonomano et al. [23] investigated a new design for trigeneration systems using centralized solar collectors. In their research, they examined high-temperature photovoltaic and thermal (PVT) panels. Because their goal was to provide high temperatures, they used parabolic solar collectors for this purpose. The collector used was capable of producing

temperatures up to 180 degrees Celsius. Therefore, a two-stage absorption chiller was used for this system. They used the zero-dimensional energy balance model on the control volume to simulate the solar collector.

Calise et al. [24] investigated a cogeneration system using solar energy. This system used PVT panels. Power, cold, heat, and water, were defined as the outputs of this system. They studied the dynamic modeling of the system and finally examined the system from an economic point of view. The system used MED technology to desalinate water, a one-stage lithium bromide absorption chiller to provide refrigeration, PVT panels to provide power and heat, and biomass auxiliary heaters.

Kegel et al. [25] investigated using a solar production system using solar energy in a high-rise building. They used TRNSYS software for their modeling. They examined energy consumption, greenhouse gas emissions by the auxiliary system, and system costs.

Calise et al. [26] modeled the solar system to produce the necessary power, purified water, and cooling, simultaneously. They used a multi-stage desalination method to produce purified water, a steam absorption chiller to produce cold water, and photovoltaic solar panels to generate power. They simulated the studied system for transient conditions and obtained the equations of the dynamic state of the system. Then they improved the system in terms of energy efficiency as well as economics. It should be noted that they used reverse osmosis to produce purified water.

Buonomano et al. [27] analyzed the energy and economics of a trigeneration system for a hotel building. The system they were using all used renewable energy. The system used geothermal energy and solar energy to supply power, heat and cold to the sample hotel. In their research, they first designed and simulated a trigeneration system in small dimensions and finally optimized the system. The system they studied included an organic Rankine cycle (ORC) with a capacity of 6 kWh, a 30 kW lithium bromide absorption chiller, a geothermal spring, and a flat panel solar collector. The thermal energy required for the Rankin organic cycle was provided by geothermal energy.

Wang et al. [28] optimized the hybrid trigeneration system using lifecycle-based solar energy. The trigeneration system they studied was used to generate power, heating and cooling. The system used solar energy and natural gas. Windeknecht and Tezchutcher [29] optimized the heat output from the cogeneration system used in a private home using a high-temperature fuel cell. They showed in their research that by reducing the storage temperature to 35 ° C, the heat output from the fuel cell could be significantly increased. This method could also reduce the initial energy consumption. Nevertheless, they illustrated that when the economic analysis was added to the thermodynamic analysis, the optimal temperature point is 45 ° C.

Verhaert et al. [30] evaluated an alkaline fuel cell micro-CHP system. They showed that for a constant mass flow rate of the coolant, in the refrigeration cycle (0.78 liters per second) the return temperature is in the range of 35 to 46 ° C.

Asensio et al. [31] modeled the CHP system based on the fuel cell using neural networks. Their purpose was to maximize system efficiency. They built an experimental prototype of their desired system with an output power of 600 w. They developed a new control system and showed that it can increase efficiency by about 8.91%.

Forresti et al. [32] experimentally investigated the cogeneration system using a fuel cell equipped with a membrane reformer. They stated that the anode pressure and relative humidity had little effect on the output voltage. However, the relative humidity and cathode pressure have a significant effect on the output voltage.

Jing et al [33] Optimized multi-objective functions of the CCHP system with solid oxide fuel cell based on economic and environmental criteria. They optimized their system for a hospital in Shanghai, China, and the results showed that the cost of generating energy per kilowatt-energy system was about $ 0.17 less than the non-optimized system.

Moradi and Mehrpooya [34] optimized the design and economic analysis of a SOFC combined system with a parabolic solar collector with the aim of providing heating, cooling and electricity to high-rise commercial towers. They used a two-effect absorption

chiller and an organic Rankine cycle. They used MATLAB software for simulation.

Chahartaghi and Alizadeh-Kharkeshi [35] performed CCHP thermodynamic analysis on a polymer membrane fuel cell as the prime mover, including a polymer membrane fuel cell, an absorption chiller, a pump and a heat storage source. The system was investigated in terms of energy, exergy and fuel storage rate. The results showed that the energy efficiency and exergy efficiency of the CCHP system were 81.5% and 54%, respectively. Exergy losses were also shown to occur most frequently in polymer membrane fuel cells. The effect of fuel cell dimensions was also studied and it was found that the larger the cell size, the higher the energy efficiency and efficiency of the chiller, but the lower the exergy efficiency. In addition, a coefficient called y was defined, which indicates that when energy production by the fuel cell is used for shooting applications, the energy efficiency is low, but in smaller values of y, the exergy efficiency increases.

Mehrpooya et al [36] examined the feasibility of using a solid oxide fuel cell to design the CCP system for a residential building. The system designed by them has 120 kW of electrical power with 45% efficiency and the overall efficiency of the system is about 60%. The payback period is calculated at 8.5 years.

You et al [37] investigated a common and advanced exergoeconomic CCHP coupled to a MED desalination system using a solid oxide fuel cell and a gas microturbine. They showed that the most exergy destruction occurs in the afterburner, which is 20.079%, followed by the SOFC with 12.986%.

Zhao et al [38] analyzed energy, exergy, environmental, economic, and multi-objective optimization of the power, heat, and refrigeration system using a PEMFC fuel cell. The results showed that by optimizing the system, energy efficiency and exergy are reduced by 5.5% and 0.77%, respectively. System costs and greenhouse gas emissions are reduced by 10% and 21.27%, respectively.

Hou et al. [39] presented a solar trigeneration system with a SOFC system for additional power production. They used absorption and electric chillers for cooling needs. They proposed an operation strategy for performance evaluation and the capacities of the main elements were optimized according to the particle swarm optimization method.

Lu et al. [40] presented a hybrid system of solar and molten carbonate fuel cell trigeneration systems. Also, the performances of the system were analyzed and energy and exergy efficiencies were evaluated. In addition, they estimated the specific carbon dioxide emission rates at different times of operation during various seasons.

As can be seen, most studies have focused on the use of one renewable energy source and the simultaneous use of two or more renewable energy sources has not received much attention. If renewable resources are not always available for various reasons, and to increase system reliability, it is always necessary to have several energy sources in the system design. Given the weaknesses of trigeneration solar systems due to the permanent lack of solar energy, which led to the need for energy storage systems that imposed additional costs on the system, in this study, an innovative hybrid system has been presented that uses solar energy and fuel cells simultaneously. This system, while being an environmentally green system, also has high operational efficiency. It can also be used in times when solar radiation is not available. The most important feature of this system is the lack of need for a solar radiant energy storage system, which has led to a reduction in return on investment and economical design. This system also has high reliability. A review of past research reveals that many studies have been conducted on trigeneration systems with primarily solar energy or fuel cells. Nevertheless, the simultaneous use of solid oxide fuel cells and solar collectors as a hybrid arrangement in order to generate heating, cooling and electricity is the main novelty of this research. Also, in the present study, the impact of some main effective parameters such as current density of fuel cell and fuel flow rate on power density, output power, fuel consumption, number of cells, electrical and thermal efficiencies, exergy destruction of the system and exergy efficiency have been investigated. Therefore, according to previous research, it is observed that the trigeneration

system with solar energy source and solid oxide fuel cell has not been studied compressively and these studies can be helpful to research to cover this gap.

Some of the main contributions and novelty of this study can be summarized below:

- Proposing a new hybrid system of trigeneration using solar collector and solid oxide fuel cell
- Presenting the energy and exergy efficiencies of this trigeneration at different operating conditions of solar irradiations
- Analyzing the impact of the current density of fuel cells on system performance
- Evaluating the carbon dioxide emission production amount at different conditions

Based on our knowledge, a review of previous research shows that so far no research has been done on the simultaneous supply of heat, cooling, and electrical energy of a building using solar energy and fuel cells without connecting the building to the electricity grid and analyzing the system from the perspective of energy, exergy and environment. Therefore this study can complement previous works.

3. Description of the system

In this research, a trigeneration system for a residential building with 4 floors and 8 units is investigated. Its total infrastructure area is 1200 m^2 for the use of 32 people. The building is located in Shahrood, which has a hot and dry climate.

In the present study, the prime mover of the trigeneration system is considered a combination of solid oxide fuel cells and photovoltaic panels. The system's output is used to supply power, hot water, and cooling and heating of residential buildings. A schematic view of the system as a whole can be seen in Fig. 1.

As shown in Fig. 1, water is first heated in solar panels by absorbing solar radiation. Then the hot water enters the fuel cell and generates power due to the methane reformer. In this process, water loses some of its heat. Then, if more water is needed for the water, it enters the auxiliary boiler and the water with the remaining heat is used first to heat the space and then to provide sanitary hot water.

It should be noted that a two-effect absorption chiller system is used to produce cooling demand. As can be seen, this system consists of three main components: a solid oxide fuel cell, solar panels and an absorption chiller. The heat source of the generator in the absorption chiller is the output hot water of the fuel cell. Also, the heat output of the generator of the absorption chiller is used for heating purposes of the building by the radiator. It should be noted that the building is not connected to the electricity grid.

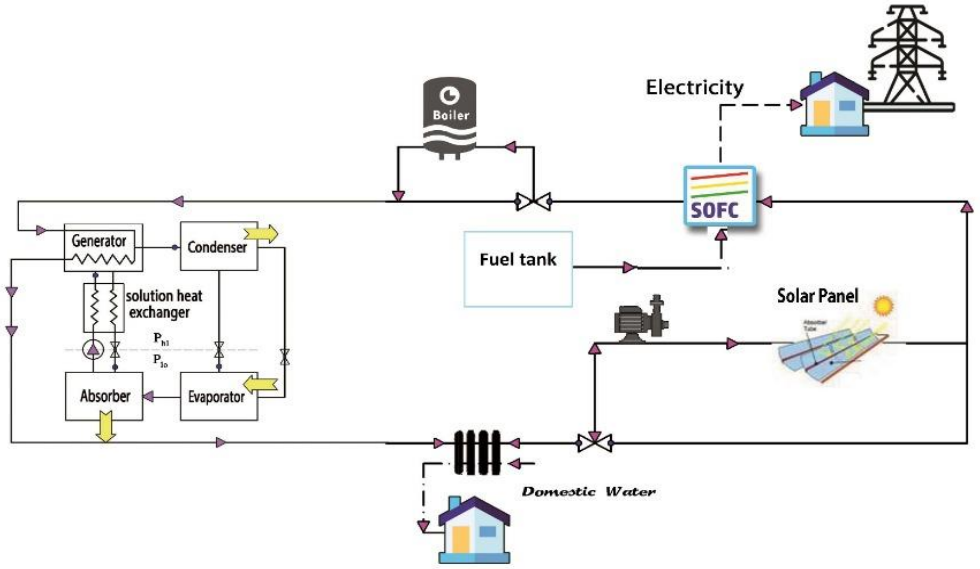

Fig. 1. Schematic view of the trigeneration system with prime mover of solid oxide fuel cell and photovoltaic plates investigated in the present study

4. System modeling

The modeling of the system and its components have been presented in this section.

4.1. Fuel cell modeling

Modeling will be performed to evaluate the electrochemical and thermal performance of a solid oxide fuel cell with methane fuel and an internal reformer at a temperature of 800 ° C. This model will be implemented using EES (Engineering Equation Solver) software. Inside the fuel cells, it is the difference between the free energy of the Gibbs formation ($\overline{\Delta G_f}$) between the reactor and the products that determine the amount of energy released during the electrochemical reaction. So we have [14]

$$\overline{\Delta G_f} = \overline{\Delta G_f}_{products} - \overline{\Delta G_f}_{reactants} \quad (1)$$

The mass values of products and reactants are often expressed in moles ($\overline{g_f}\left(\frac{J}{mol}\right)$). The general reaction in a SOFC fuel cell that runs on methane is given as[14]

$$CH_4 + 2O_2 \rightarrow 2H_2O + CO_2 \quad (2)$$

Products contain two moles of water and one mole of carbon dioxide, while reactants contain one mole of methane and two moles of oxygen. Gibbs free energy changes for one mole of reactants are expressed as [14]

$$\overline{\Delta g_f} = \overline{g_f}\ of\ products - \overline{g_f}\ of\ reactants = \left(\left(\overline{g_f}\right)_{H_2O} + \frac{1}{2}\left(\overline{g_f}\right)_{CO_2}\right) - \left(\left(\overline{g_f}\right)_{O_2} + \frac{1}{2}\left(\overline{g_f}\right)_{CH_4}\right) \quad (3)$$

For one mole of methane injected into the SOFC, 8 electrons can be released and circulated in the circuit. Therefore[15],

$$CH_4 + 4O^{2-} \rightarrow 2H_2O + CO_2 + 8e^- \quad (4)$$

Actual operating voltage (V_{cell}) is less than the ideal voltage due to voltage drop. Actual operating voltage (V_{cell}) is calculated using[15]

$$V_{cell} = E_{OCV} - \Delta V_{ohm} - \Delta V_{act} - \Delta V_{trans} \quad (5)$$

Activation losses (ΔV_{act}), due to slow reactions, occur on the electrolyte surface and are equal to the sum of cathode and anode activation losses and are calculated as[15]

$$\Delta V_{act} = \Delta V_{act,anode} + \Delta V_{act,cathode} \quad (6)$$

The total input energy in watts ($\dot{Q}_{CH_4}$) is calculated using[15]

$$\dot{Q}_{CH_4} = \frac{\dot{W}_{elec,DC}}{\eta_{cell}} \quad (7)$$

where, $\dot{W}_{elec,DC}$ is the DC output power of the solid oxide fuel cell and η_{cell} is the cell efficiency. The mass flow rate of methane entering the SOFC stack is calculated as [15]

$$\dot{m}_{CH_4} = \frac{\dot{Q}_{CH_4}}{LHV_{CH_4}} \quad (8)$$

It should be noted that the low calorific value for methane fuel is $5 \times 10^7 \frac{J}{kg}$. It should also be noted that the low calorific value for methane fuel is $5 \times 10^7 \frac{J}{kg}$.The total AC power output of the fuel cell stack is calculated in Watts using[13]

$$\dot{W}_{elec,AC} = \left(\dot{W}_{elec,DC} - \dot{W}_{BoP}\right).\eta_{inverter}. \quad (9)$$

4.2. Modeling of solar panels

In this section, the aim is to determine the amount of absorption of solar radiation by solar panels and the amount of heat produced by it. With this value, the water temperature at the output of the solar panel can be determined.

The amount of radiation removed for each surface represented by i (i = c, os, r) must be calculated using[21]

$$B_c = \varepsilon_c \sigma T_c^4 + \left(1-\alpha_c\right)\left(B_c F_{A_c-A_c} + B_{os} F_{A_c-A_{os}} + B_r F_{A_c-A_r}\right), \quad (10)$$

$$B_r = \varepsilon_r \sigma T_r^4 + \left(1-\alpha_r\right)\left[B_c F_{A_r-A_c} + B_{os} F_{A_r-os} + B_r F_{A_r-A_r} + \left(1-\alpha_c\right)\dot{I}\frac{A_c}{A_r}\right] \quad (11)$$

and

$$B_{os} = \sigma T_0^4 \quad (12)$$

as a function of temperature. In Eqs. (10-12), if the absorber is assumed to be a flat plate, then $F_{A_r-A_r} = 0$. Then, according to the reciprocity rule, we will also have

$$A_r F_{A_r-A_c} = A_c F_{A_c-A_r}. \quad (13)$$

Other required shape coefficients can also be calculated using the law of reciprocity as

well as the summation rule for each level as[22]

$$F_{A_c-A_{os}} = 1 - F_{A_c-A_c} - F_{A_c-A_r}, \quad \text{and} \tag{14}$$

$$F_{A_r-A_{os}} = 1 - F_{A_r-A_c} \ . \tag{15}$$

In this way, Eqs. (14-15) can be solved analytically, and using the results, Bi can be obtained for the desired geometry. With Bi, the temperature can be calculated at any given time.

It is also possible to calculate the amount of solar radiation from other objects (emitted by the environment) as well as direct radiation from the sun using [23]

$$H_c = B_c F_{A_c-A_c} + B_{os} F_{A_c-A_{os}} + B_r F_{A_c-A_r} + \dot{\mathrm{I}}, \tag{16}$$

and

$$H_r = B_c F_{A_r-A_c} + B_{os} F_{A_r-A_{os}} + B_r F_{A_r-A_r} + (1-\alpha_c)\dot{\mathrm{I}} \frac{A_c}{A_r}. \tag{17}$$

Also, the amount of total radiant heat transfer in a gray surface can be calculated from[21]

$$\dot{Q}_c = \left[\alpha_c \left(\dot{\mathrm{I}} + B_c F_{A_c-A_c} + B_{os} F_{A_c-A_{os}} + B_r \frac{A_r}{A_c} F_{A_r-A_c} \right) - \varepsilon_c \sigma T_c^4 \right] A_c, \quad \text{and} \tag{18}$$

$$\dot{Q}_r = \left[\alpha_r \left(B_c F_{A_r-A_c} + B_{os} F_{A_r-A_{os}} + (1-\alpha_c)\dot{\mathrm{I}} \frac{A_c}{A_r} \right) - \varepsilon_r \sigma T_r^4 \right] A_r \tag{19}$$

The shape coefficient according to the geometry of the problem can be calculated using [24]

$$F_{A_r-A_c} = \frac{1}{A_r} \int_{A_r} \int_{A_c} \frac{\cos\beta_r \cos\beta_c}{\pi r^2} dA_c dA_r. \tag{20}$$

Three more equations are now needed to calculate the output temperature of the concentrator, receiver, and coil as a function of temperature. Therefore, the first law of thermodynamics must be written for each of the volumes of the mentioned controls. As a result, we have[24]

$$\frac{dT_c}{dt} = \left\{ \dot{Q}_c - \dot{Q}_{c,w} \right\} \frac{1}{m_c C_c} \tag{21}$$

where $\dot{Q}_{c,w}$ is given as[23]

$$\dot{Q}_{c,w} = U_{c,w} A_{c,w} \left(T_c - T_0 \right), \quad \text{and} \tag{22}$$

Tc represents the concentration temperature [21]. Also,

$$\frac{dT_r}{dt} = \left\{ \dot{Q}_r - \dot{Q}_{r,w} - \dot{Q}_{sp} \right\} \frac{1}{m_r C_r} \tag{23}$$

Where

$$\dot{Q}_{r,w} = U_{r,w} A_{r,w} \left(T_r - T_0 \right), \dot{Q}_{sp} = U_{r,sp} A_{r,sp} \left(T_r - T_{sp} \right). \tag{24}$$

In Eqs. (23) and (24), T_r is the temperature of the receiver [21], and T_{sp} is given by

$$T_{sp} = \left\{ \dot{Q}_{sp} + \dot{Q}_{sps} - \dot{W}_{fr,sp} \right\} \frac{1}{m_{sp,s} C_s} \tag{25}$$

where $\dot{Q}_{sps}$ is given by[21]

$$\dot{Q}_{sps} = \dot{m}_{sp} c_s \left(T_{ct} - T_{sp} \right) \tag{26}$$

In Eq. (25), T_{sp}represents the temperature of the coil inside the receiver, assuming that the agent does not change phase.

Also, the pressure drop in the coil can be determined from[21]

$$\dot{W}_{fr,i} = \dot{m}_i \Delta P_i / \rho_{fluid} \tag{27}$$

in which

$$\Delta P_i = 2 f \frac{L_i}{D_i} \rho_{fluid} u_i^2. \tag{28}$$

We also know that $u_i = \frac{\dot{m}_i}{\rho_{fluid} A_{i,ts}}$, where the subtitle i indicates the local position.

4.3. Double-effect absorption chiller equations

The amount of refrigeration to be produced is indicated by the symbol $\dot{Q}_E$ by writing the energy conservation equation for the evaporator. Thus, we will have [27]

$$\dot{Q}_E = \dot{m}_r \left(h_9 - h_8 \right) = \dot{m}_E \left(h_c - h_d \right) \tag{29}$$

The exergy of the refrigeration system, $\dot{E}_E$, is calculated as[25]

$$\dot{E}_E = \dot{Q}_E \left(\frac{T_0 - T_E}{T_E} \right). \quad (30)$$

4.4. Total system equations

The total efficiency of the system and the total exergy efficiency of the system are calculated as[25]

$$\eta_{overall} = \frac{W_{SOFC} + W_{collector} - W_{cond} + Q_{Recover\ heat}}{m_{fuel} \times LHV_{fuel}} \quad (31)$$

$$\eta_{exergy.overall} = \frac{E_{SOFC} + E_{collector} - E_{cond} + Q_{Recover\ heat}}{m_{fuel} \times E_{fuel}}, and \quad (32)$$

$$\eta_{exergy.overall} = \frac{E_{SOFC} + E_{collector} - E_{cond} + Q_{Recover\ heat}}{m_{fuel} \times E_{fuel}} \quad (33)$$

4.5. Environmental equations

In this system, due to the high sensitivity of fuel cell components, the inlet fuel must have the lowest amount of sulfur, which prevents the production of sulfuric acid formations and other emissions in the exhaust gases. CO, CO_2 and NOx are considered the main pollutants. Experimental data show that the amount of CO and NOx emitted from the solid oxide fuel cell stack is negligible. Therefore, it is assumed that the emission of these two pollutants is only from the combustion chamber in case of fuel injection into the combustion chamber and their emission depends on the combustion characteristics such as the flame adiabatic temperature which can be estimated using[27]

$$T_{pz} = A\delta^a \exp\left[\beta(\delta + \lambda)^2\right] \pi^{x^*} \theta^{y^*} \psi^{z^*}. \quad (34)$$

In the above equation, π and θ are dimensionless pressure and temperature and ψ is the atomic ratio of hydrogen to carbon. Ø = δ for 1≥Ø and for1≤Ø is equal to δ = Ø-0.7. The coefficients x, y and z are also calculated using the following equations [27]:

$$x^* = a_1 + b_1\delta + c_1\delta^2 \quad (35)$$

$$y^* = a_2 + b_2\delta + c_2\delta^2 \quad (36)$$

$$z^* = a_3 + b_3\delta + c_3\delta^2 \quad (37)$$

A ،a ،β ،λ ،a_i ،b_i and c_i are fixed values. The amount of CO and NOx emissions from the combustion chamber in terms of grams per kilogram of fuel can be calculated through the following equations[25]:

$$m_{NO_x} = \frac{0.15 \times 10^{16} \tau^{0.5} exp\left(\frac{-71100}{T_{PZ}} \right)}{P_3^{0.05} \left(\frac{\Delta P_{in}}{P_{in}} \right)^{0.5}} \quad \text{and} \quad (38)$$

$$m_{CO} = \frac{0.179 \times 10^{9} \exp\left(\frac{7800}{T_{PZ}} \right)}{P_3^{2} \tau \left(\frac{\Delta P_{in}}{P_{in}} \right)^{0.5}} \quad (39)$$

where τ is the ignition time (about 2 milliseconds), T_{PZ} is the initial temperature of the ignition zone, P_3 is the inlet pressure to the combustion chamber and $\frac{\Delta P_{in}}{P_{in}}$ is the dimensionless pressure drop of the combustion chamber.

The amount of CO_2 released into the atmosphere, which is one of the main products of the combustion reaction, is evaluated according to the combustion equations in the combustion chamber.

The amount of CO_2 is evaluated by[25]

$$\dot{m}_{co_2} = 44.01x \frac{\dot{m}_{fuel}}{m_{fuel}} \quad (40)$$

where x is the molar fraction of carbon in the fuel. The cost of CO_2 emissions is defined as [25]

$$\dot{C}_{env} = Cco_2 \dot{m}_{co_2} \quad (41)$$

In the above equation, CO_2 is considered equal to (0.0024 $)/(kg$CO_2$) in the calculations.

5. The system conditions

This residential building has 4 floors and 8 units. Its total infrastructure area is 1200 m^2 for the use of 32 people. The building is located in Shahrood, which has a hot and dry climate. In calculating the electric charge, the consumption of system pumps and absorption chillers is also considered. The main electrical consumption of the building is calculated using the ASME standard and presented in Table 1 [41]. According to the demand rate of 0.76, the

amount of electrical power required during peak hours is equal to 30 kW. The amount of heat power required for heating in winter is 52.9 W/m^2 W/m^2, 63.5 kW. The required cooling capacity is 117.8 W/m^2, which means that the total cooling required for the building in summer is 141.3 kW. Assuming the use of an absorption chiller with a coefficient of performance of 0.7, the required amount of heat will be 201.9 kW. The amount of heat required for hot water consumption is 28.7 kW.

The study is performed for the most critical point. This point includes 15 August at 15:00. In this situation, the ambient temperature is equal to 32℃ and the intensity of solar radiation is 1100 W/m^2. Modeling is performed for the steady-state condition.

The technical specifications of the proposed fuel cell are shown in Table 2.

The values related to the thermodynamic parameters of the problem including the temperature of different points as well as the efficiency of the components are considered according to Table 3.

6. Working method and validation

The system of equations presented for the analysis of solid oxide fuel cell and solar collector is mathematically certain, however, in addition to the boundary conditions and parameters mentioned in the text, the operating conditions of the fuel cell need to be specific to solve these equations. These operating parameters include the molar flow rate of the fuel flow or fuel consumption, the molar flow rate of the airflow or the amount of excess air, and the output voltage or density distribution of the electric current of the fuel cell. The equations for the solar collector are also definite. Therefore, all equations in EES software are solved in static mode. In each case, by considering an unknown and entering the value of other parameters as known, the output of the software is taken, which can be seen in the results section.

Figure 2 shows the problem-solving flowchart.

Table 1. The amount of energy consumption of different parts of the sample building

consumable	Consumption rate (units)	Units
Lighting	43	$(\frac{W}{m^2})$
Television	158	W
Refrigerator	140	W
Iron	940	W
Washing machine	345	W
Personal computer	225	W

Table 2. Fuel cell technical specifications [38]

Parameter	Amount (units)
Area of each cell	1038.25 (cm^2)
The length of each cell	160 (cm)
Diameter of each cell	2.5 (cm)
current density	3500 $(\frac{A}{m^2})$
Fuel consumption coefficient	0.87
Working temperature	1250 (Kelvin)
Work pressure	3 bar
Inlet airflow	100 (km / h)
Inlet fuel flow	10.92 (km / h)

Table 3. Thermodynamic data of the problem

η_{PP}	0.35	$T_0(C^o)$	20
η_g	0.87	$T_{room,sum}(C^o)$	27
η_b	0.83	$T_{room,win}(C^o)$	23
η_{CHP}	0.88	$T_{exhaust}(C^o)$	1100
ε_{FCU}	0.86	$T_{db,sum}(C^o)$	40
ε_{wh}	0.87	$T_{db,win}(C^o)$	-6.7
Solar radiation	1150 $(\frac{W}{m^2})$		

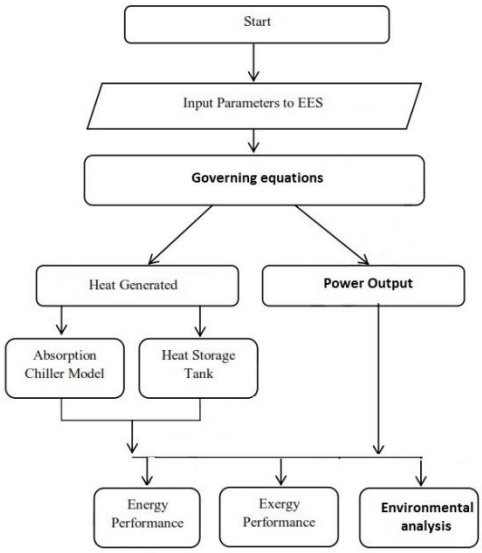

Fig. 2. Flowchart of process analysis

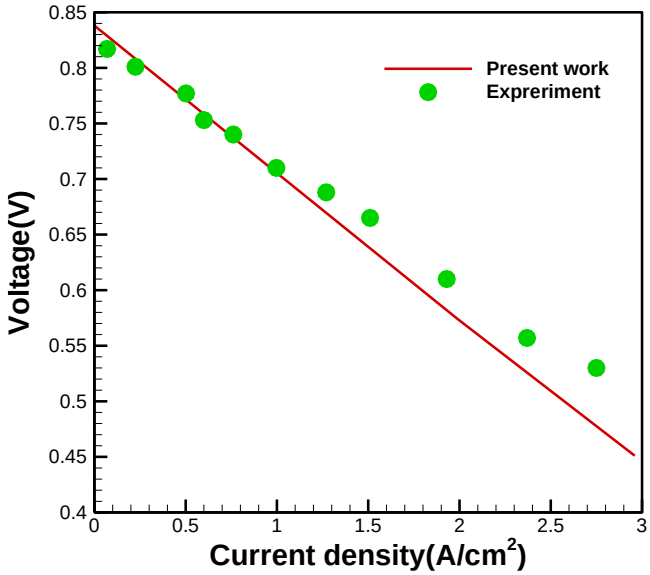

Fig. 3. Validation of the model for SOFC

To validate the model developed in this research, the results of the electrochemical model output are compared to the empirical results according to Fig. 3. The operating temperature of SOFC is assumed to be 800 ° C and the combined fuel input is considered to be 97% hydrogen and 3% water [20].

7. Results and discussion

Figure 4 shows the changes in power density and voltage relative to current density. As can be seen, with increasing current density, the power density also increases because power is directly related to the square of the current. On the other hand, voltage is inversely related to current. Hence, as the current increases, the voltage decreases linearly.

Considering that the power of each SOFC unit is equal to 570 kW and according to the diagram shown, the area of each fuel cell is about 200 cm^2. According to these values, the required number of fuel cells can be calculated. Table (4) shows the electrochemical results and system efficiencies.

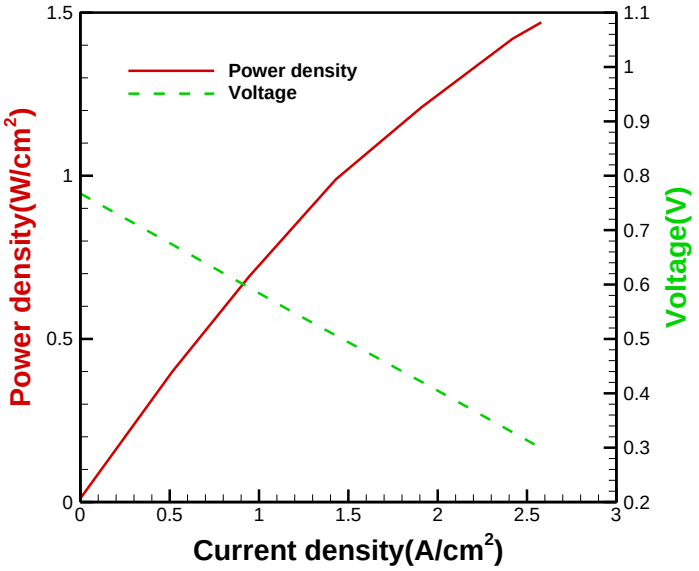

Fig. 4. Changes in power density and voltage with respect to the current density

Table 4. Electrochemical results and efficiency

Parameter	Value	Parameter	Value
U_f	0.8401	N_{cell}	35000
I_{SOFC}	689150(A)	$\eta_{net,overal,LHV}$	86.90%
V	0.838(V)	$\eta_{elec,SOFC}$	46.77 %
J	0.150($\frac{A}{Cm^2}$)	$\eta_{net,LHV}$	53.97%

Figure 5 shows the changes in stack power relative to the current density at different operating temperatures of the fuel cell. It shows that higher operating temperatures lead to a rise in power output. It is also observed that with increasing current density, first the fuel cell production capacity increases, and after reaching a maximum point, the production power capacity decreases with a further increase of current density. As the operating temperature of the fuel cell increases, the optimum point for the current density also increases.

Figure 6 shows the changes in electrical efficiency concerning current density. It is observed that the decrease in electrical efficiency occurs linearly with increasing the current density for the fuel cell and the whole system. Because the electrical efficiency of the system is directly a function of the electrical efficiency of the fuel cell. The electrical efficiency of the fuel cell is also linear and inversely related to the current density.

Current density has an impact on power and voltage and natural gas flow rate. These factors affect the system's overall electrical efficiency. The SOFC electrical efficiency is declined with increasing the current density. As the current density increases the system's electrical efficiency rises to its maximum value and then reduces. The highest electrical efficiency of the whole system is about 53.97%. Figure 7 shows the effect of operating temperature (T_w) on the solar thermal efficiency (η_c).

The thermal efficiency of the solar collector decreases with an increasing amount of Tw. As the inlet temperature increases from 500 ° C to 1150 ° C, the thermal efficiency of the system decreases from about 0.87 to 0.82 since by increasing the working temperature, the amount of heat loss increases.

Figures 8 and 9 show the changes in total exergy elimination and total exergy efficiency for the system for different values of fuel mass flow rate.

Figure 8 shows that with increasing flow

rate, the rate of exergy destruction increases, the main reason being the increase in operating temperature of the system due to the increase in flow rate and also the increase in the heat loss rate of solid oxide fuel cells.

Figure 9 also shows that as the flow rate increases, the amount of exergy efficiency decreases due to the increase in the rate of exergy destruction, which was described. Because the main factor in reducing exergy efficiency is increasing the exergy destruction in the system.

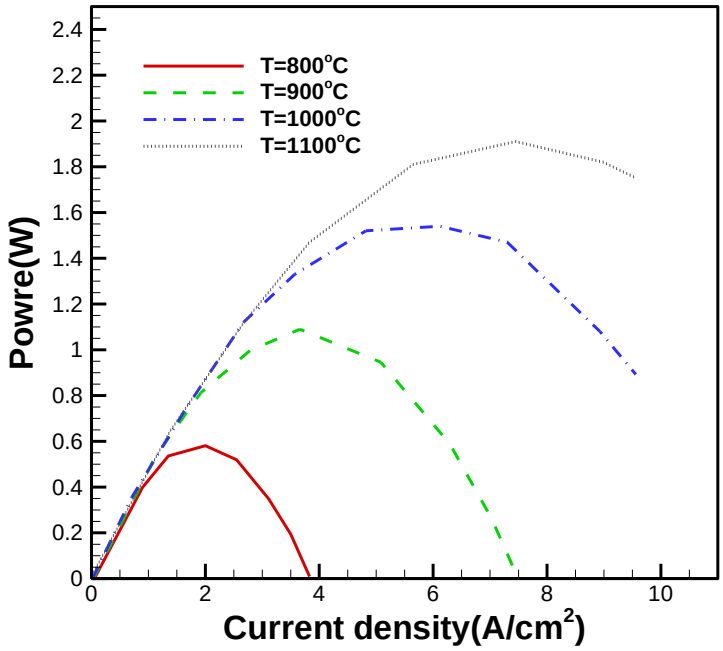

Fig. 5. Changes in the power output at different operating temperatures

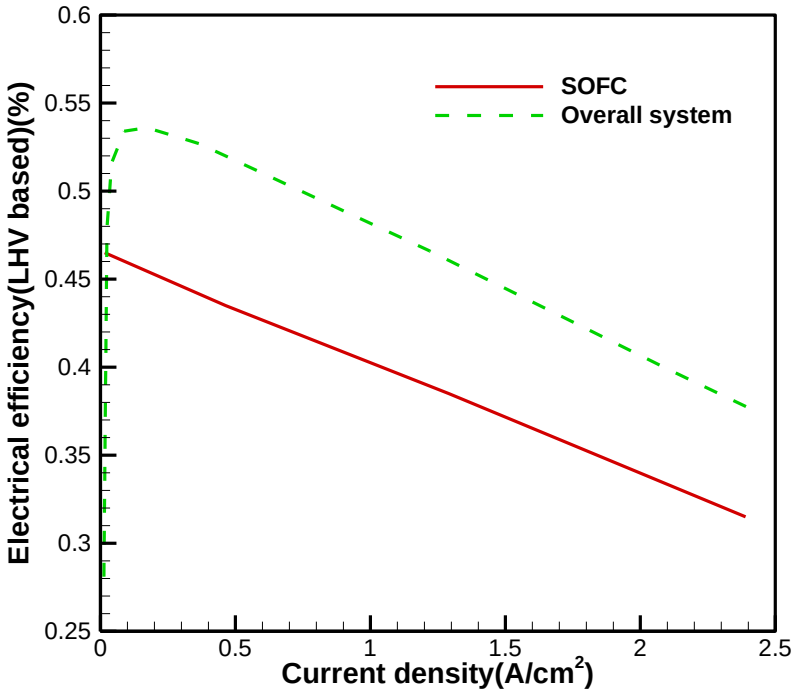

Fig. 6. Variable electrical efficiency with current density

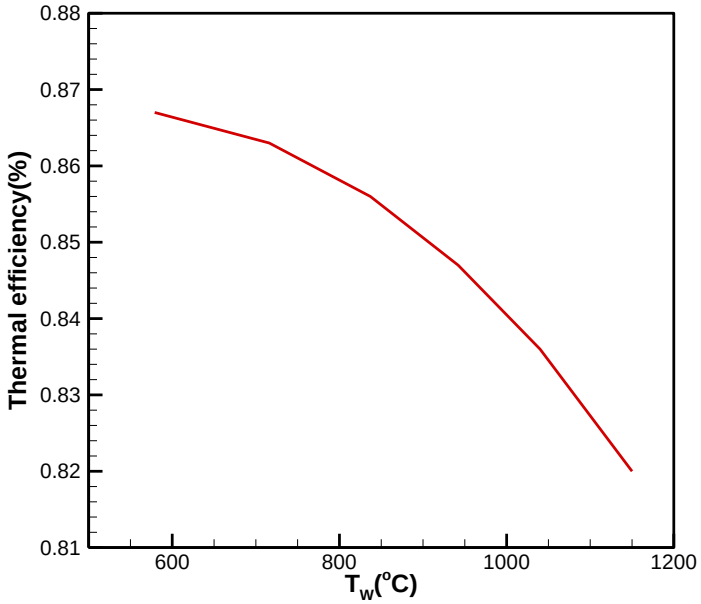

Fig. 7. Thermal efficiency changes of the solar collector with T_w

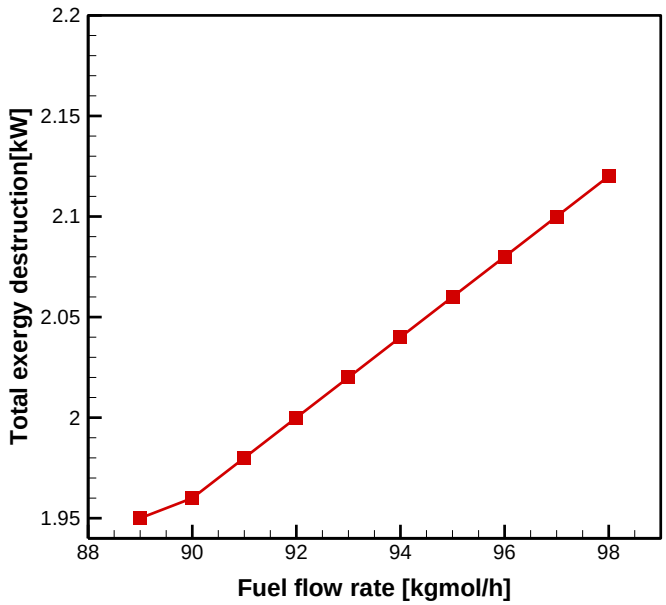

Fig. 8. Total exergy destruction changes for the system for different fuel mass flow rates

As shown in Fig. 8, the rate of exergy destruction increases with increasing inlet fuel flow rate. Because according to Eq (32), exergy destruction and exergy efficiency have an inverse relationship with the mass flow rate of the input fuel. increasing the flow rate of incoming fuel means increasing the share of fuel cells in the production of electricity and heat relative to solar energy, and this leads to increased energy consumption and thus reduces exergy efficiency and increases exergy destruction. By increasing the share of solar energy in the production of electrical and thermal energy of the system, the flow rate of fuel entering the fuel cell is reduced and as a result, thermal, electrical, and total energy efficiencies and total exergy efficiency are improved.

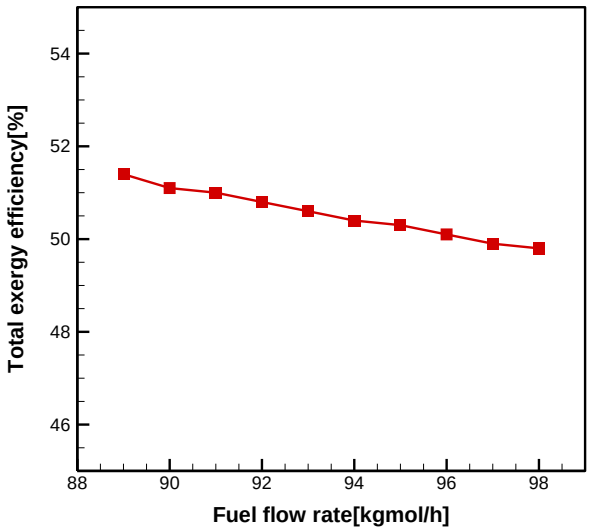

Fig .9. Total exergy efficiency changes for the system for different values of the mass flow rate of the fuel

Figure 9 shows that as the fuel mass flow rate increases, the exergy efficiency decreases almost linearly. In fact, with increasing fuel flow rate, the operating temperature of the fuel cell increases, and as a result, the destruction of the exergy due to temperature irreversibility increases, and consequently, the efficiency of the exergy decreases.

Figure 10 shows the energy efficiency changes for the trigeneration system for different fuel mass flow rates. As shown in Fig.10, as the fuel mass flow rate increases, the electrical efficiency and overall efficiency of the system decrease. But this reduction in efficiency is not linear, unlike the reduction in exergy. Because with increasing the mass flow rate of the fuel, the operating temperature of the fuel cell increases. Hence the heat loss increases and as a result, the efficiency decreases. Nevertheless, unlike the relationship between exhaust extinction and temperature irreversibility, which is linear, the relationship between temperature loss and temperature is not linear hence the reduction occurs nonlinearly. It is also observed that by increasing the fuel flow rate by 5(Kg.Mol/h), the electrical efficiency decreases by about 5%, and the total efficiency by about 10%, while the exergy efficiency decreases by less than 2%.

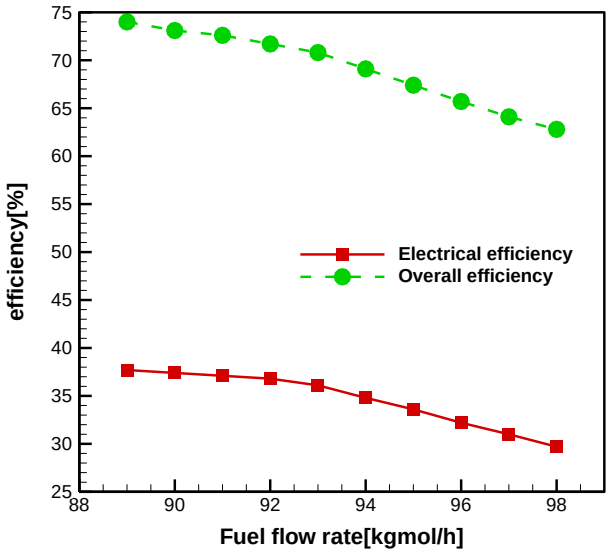

Fig. 10. Energy efficiency for the trigeneration system studied for different fuel mass flow rates and quantities

Figure 11 shows the effect of solar radiation intensity on thermal efficiency, assuming that the parameters related to solid oxide fuel cells are constant.

According to Fig.11, it can be seen that with increasing the intensity of solar radiation, its thermal efficiency increases with the rise of the intensity of solar radiation leading to more heat absorption by the collector and thus more efficiency of the solar collector.

Figure 12 shows the changes in the total exergy efficiency system relative to the intensity of solar radiation.

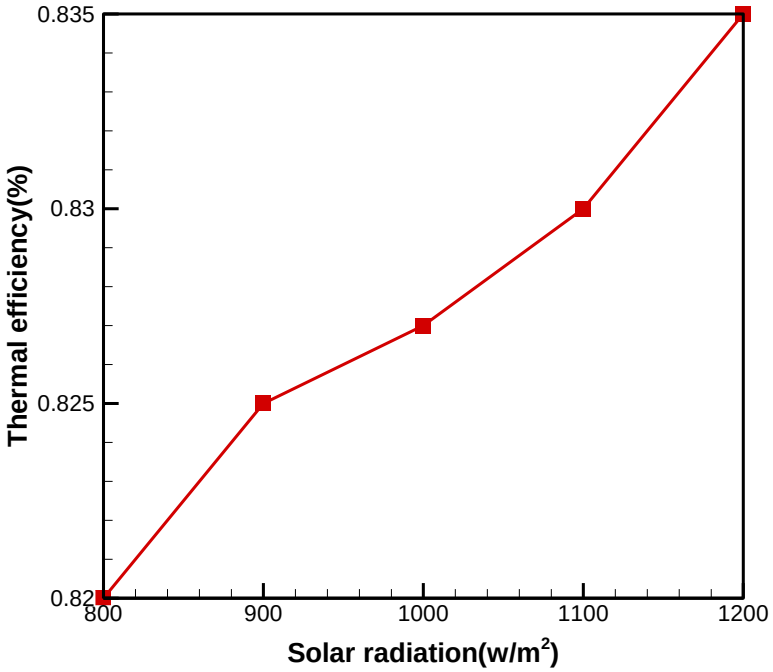

Fig. 11. Thermal efficiency changes of the solar collector with solar radiation

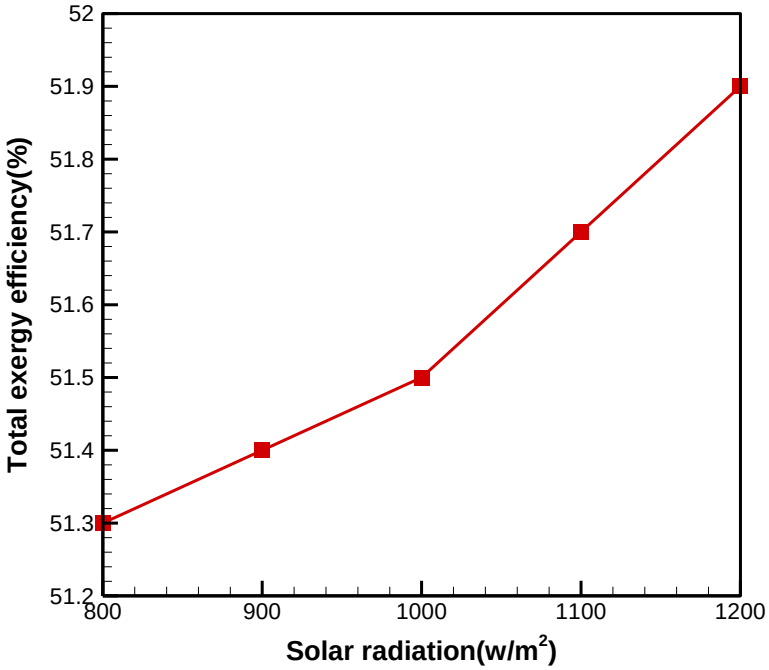

Fig.12. Total system exergy efficiency changes for different solar radiation

As shown in Fig.12, with increasing solar radiation intensity, as the thermal performance of the solar collector improves, the system's total exergy efficiency also increases. It should be noted that this study assumes that the efficiency of the solar collector is constant for all solar radiation. Also, the effect of the decrease in the efficiency of the solar collector performance with the increase of the collector temperature has not been considered. Therefore, increasing solar radiation leads to increased electricity production by the photovoltaic panel as well as more heat transfer to the operating fluid, thus improving the system's exergy efficiency.

Regarding the environmental analysis of cycle performance, the results presented in various studies show that the amount of carbon monoxide gas and nitrogen monoxide produced by the fuel cell is low and therefore only the environmental impact of carbon dioxide gas should be investigated. Due to the fact that the amount of carbon dioxide emission coefficient is calculated to be 358.2, which is very small and desirable compared to conventional hybrid systems. To optimize the proposed hybrid system based on a solid oxide fuel cell, two main parameters including exergy efficiency and carbon dioxide emission coefficient are considered. The first parameter is directly related to the net output work and should be maximized and the second parameter should be minimized.

According to Fig.13, the maximum amount of net output work and consequently the highest amount of exergy efficiency for the proposed system is obtained at point A, where the carbon dioxide emission coefficient is minimal. Hence point A can be selected as the design point.

As the output power of the unit increases, its energy efficiency and exergy increase, and as a result, the amount of pollutant production decreases according to the amount of power produced(MWh).

Figure 14 shows the effect of current density on carbon dioxide emissions.

Figure 14 shows that with increasing the current density, the amount of carbon dioxide emissions increases. Because with increasing the current density, the amount of fuel cell exergy losses increases, and therefore the efficiency of the fuel cell and the whole system decreases, which means that to produce a certain power, more fuel is needed, which means an increase of emissions of pollutants.

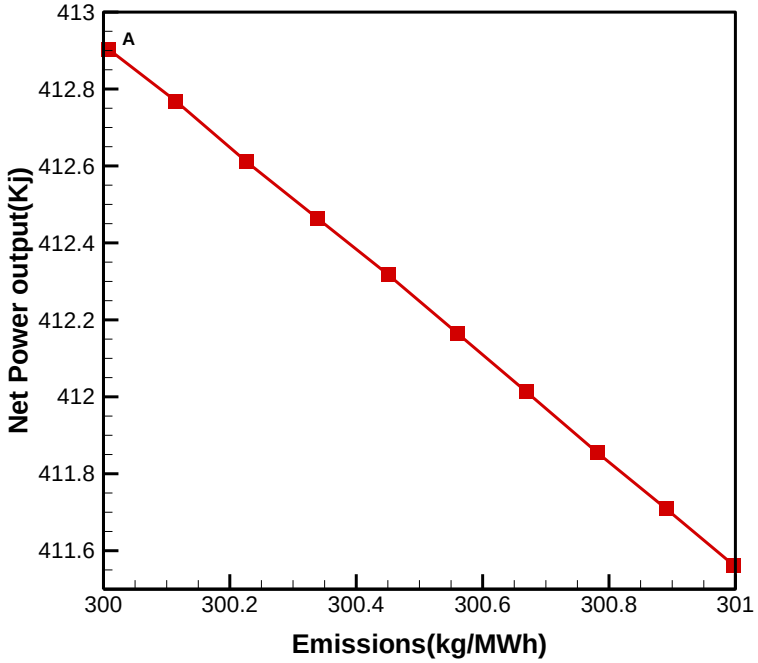

Fig.13. Influence of carbon dioxide emission coefficient on the net work output of the cycle in the optimal point design

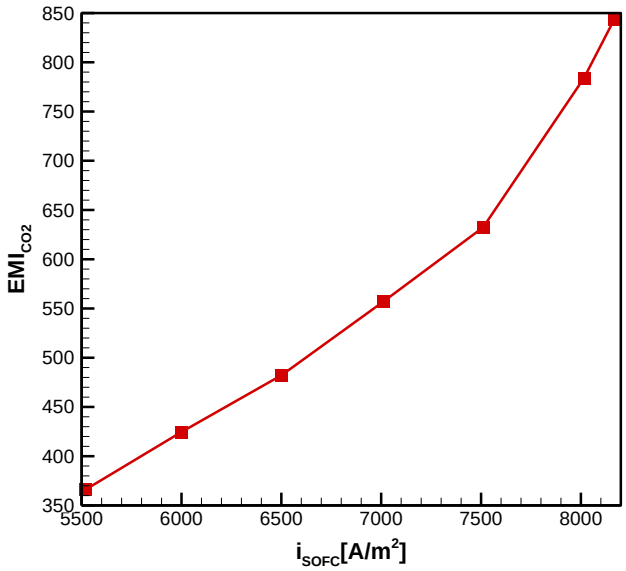

Fig.14. Influence of current density on carbon dioxide emissions

According to the figure, it can be seen that with increasing current density, the emission of carbon dioxide increases because the energy efficiency decreases. With changes in the gas emission density of carbon dioxide per megawatt, it increases from 375 kg / MWH to 848 kg / MWH.

6. Conclusion

In this research, a new trigeneration system with the prime mover of solid oxide fuel cells and solar energy has been analyzed. For this purpose, a residential building is used to supply the energy demand. The heating, cooling, and power required for the building have been calculated. The energy conservation equations have been derived for each component of the system, and the energy and exergy performances of the system have been evaluated. Also, the impacts of fuel flow rate, solar radiation intensity and current density on the performance of the system have been evaluated. The most important results can be categorized as follows:

- The total value of electrical power produced by the system in summer and spring is about 1184.5 kW and in winter and autumn is 1121.7 kW.
- The whole annual electrical energy generation of the system is about 9921112 kWh and 1301.2 MWh of thermal energy is collected by solar cells per year.
- The SOFC electrical efficiency is equal to 46.77% and the whole system is equal to 53.97%.
- The thermal efficiency of the whole system is equal to 86.90% which is higher than conventional systems.
- By using solar energy, the designed system can provide heat and cold loads for the building well and the efficiency of the trigeneration system is much higher than similar systems.
- At higher values of the current density, the carbon dioxide emission increases.
- The carbon dioxide emission coefficient is 358.2, which is very low and desirable compared to fossil fuel systems.

Reference

[1] Ahmadi, P., Rosen M. A., Dincer, I., "Multi-objective exergy-based optimization of a polygeneration energy system using an evolutionary algorithm," *Energy,* vol. 46, pp. 21-31, 2012.

[2] Ebrahimi, M. "The environ-thermo-economical potentials of operating gas turbines in industry for combined cooling, heating, power and process (CCHPP)," *Journal of cleaner production*, vol. 142, pp. 4258-4269, 2017.

[3] Szega, M., Żymełka, P., & Janda, T. (2021). Improving the accuracy of electricity and heat production forecasting in a supervision computer system of a selected gas-fired CHP plant operation. *Energy*, 122464.

[4] Stark.M, et al. "Steam storage systems for flexible biomass CHP plants-Evaluation and initial model based calculation." Biomass and Bioenergy 128 (2019): 105321.

[5] Rusanov. A, et al. "Heating modes and design optimization of cogeneration steam turbines of powerful units of combined heat and power plant." Energetika 65.1 (2019).

[6] Mosaffa, A. H., Z. Ghaffarpour, and L. Garousi Farshi. "Thermoeconomic assessment of a novel integrated CHP system incorporating solar energy based biogas-steam reformer with methanol and hydrogen production." Solar Energy 178 (2019): 1-16.

[7] Villarini.M, et al. "Sensitivity analysis of different parameters on the performance of a CHP internal combustion engine system fed by a biomass waste gasifier." Energies 12.4 (2019): 688.

[8] Sheykhi. M, et al. "Performance investigation of a combined heat and power system with internal and external combustion engines." Energy Conversion and Management 185 (2019): 291-303.

[9] Elsner, Witold, et al. "Experimental and economic study of small-scale CHP installation equipped with downdraft gasifier and internal combustion engine." Applied Energy 202 (2017): 213-227.

[10] González-Pino, I., et al. "Modelling and experimental characterization of a Stirling engine-based domestic micro-CHP device." Energy Conversion and Management 225 (2020): 113429.

[11] Cardozo.E, and Malmquist.A "Performance comparison between the use of wood and sugarcane bagasse pellets in a Stirling engine micro-CHP system." Applied Thermal Engineering 159 (2019): 113945.

[12] Qiu, Songgang, et al. "Development of an advanced free-piston Stirling engine for micro combined heating and power application." Applied Energy 235 (2019): 987-1000.

[13] Chahartaghi.M, Sheykhi.M " Thermal modeling of a trigeneration system based on beta-type Stirling engine for reductions of fuel consumption and pollutant emission" Journal of Cleaner Production 205 (2018): 145-162.

[14] Chahartaghi.M, Sheykhi.M " Energy, environmental and economic evaluations of a CCHP system driven by Stirling engine with helium and hydrogen as working gases" Energy 174 (2019): 1251-1266.

[15] Yu, Dongmin, et al. "Dynamic multi agent-based management and load frequency control of PV/fuel cell/wind turbine/CHP in autonomous microgrid system." Energy 173 (2019): 554-568.

[16] Pashaei-Didani. H, et al. "Optimal economic-emission performance of fuel cell/CHP/storage based microgrid." International Journal of Hydrogen Energy 44.13 (2019): 6896-6908.

[17] Fan, Xiaochao, et al. "Multi-objective optimization for the proper selection of the best heat pump technology in a fuel cell-heat pump micro-CHP system." Energy Reports 6 (2020): 325-335.

[18] Chahartaghi M., et al." Energy and exergy analyses of a combined cooling, heating and power system with prime mover of phosphoric acid fuel cell with organic Rankine cycle."Applied Thermal Engineering Volume 193, 5 July 2021, 116989

[19] Pilpola, Sannamari, and Peter D. Lund. "Different flexibility options for better system integration of wind power." Energy Strategy Reviews 26 (2019): 100368.

[20] Li, Yaowang, et al. "Combined heat and power dispatch considering advanced adiabatic compressed air energy storage for wind power accommodation." Energy Conversion and Management 200 (2019): 112091.

[21] Tang, Lanxi, et al. "Comparison of Fuel-saving Effect Between Heat Accumulator and Electric Boiler Used for Wind Power Accommodation in CHP Plant." 2020 12th IEEE PES Asia-Pacific Power and Energy Engineering Conference (APPEEC). IEEE, 2020.

[22] Calise. F, M.Dentice d'Accadia, L.Vanoli, "Design and dynamic simulation of a novel

solar trigeneration system based on hybrid photovoltaic/thermal collectors (PVT)", Energy Conversion and Management 60 (2012) 214–225.

[23] Buonomano.A,Calise.F , M.Dentice d'Accadia , L.Vanoli, "A novel solar trigeneration system based on concentrating photovoltaic/thermal collectors. Part 1: Design and simulation model", Energy 61 (2013) 59e71.

[24] Calise. F, M.Dentice d'Accadia, A.Piacentino, "A novel solar trigeneration system integrating PVT (photovoltaic/ thermal collectors) and SW (seawater) desalination: Dynamic simulation and economic assessment", Energy 67 (2014) 129e148.

[25] Kegel.M, J.Tamasauskas,R.Sunye," Solar Thermal Trigeneration System in a Canadian Climate Multi-unit Residential Building", Energy Procedia Volume 48, 2014, Pages 876–887.

[26] Calise, F.; d'Accadia, M.D.; Piacentino, A. A novel solar trigeneration system integrating PVT (photovoltaic/thermal collectors) and SW (Seawater) desalination: Dynamic simulation and economic assessment. Energy 2014, 67, 129–148.

[27] A.Buonomano, F.Calise, A.Palombo, M.Vicidomini, "Energy and economic analysis of geothermal–solar trigeneration systems: A case study for a hotel building in Ischia", Applied Energy 138 (2015) 224–241.

[28] Wang. J, Yang. Y, T.Mao, Jun Sui, Hongguang Jin, "Life cycle assessment (LCA) optimization of solar-assisted hybrid CCHP system", Applied Energy 146 (2015) 38–52.

[29] Windeknecht.M, and P.Tzscheutschler. "Optimization of the heat output of high temperature fuel cell micro-CHP in single family homes." Energy Procedia 78 (2015): 2160-2165.

[30] Verhaert.I, Grietus.M, and M.De Paepe. "Evaluation of an alkaline fuel cell system as a micro-CHP." Energy conversion and management 126 (2016): 434-445.

[31] Asensio, F. J., et al. "Fuel cell-based CHP system modeling using Artificial Neural Networks aimed at developing techno-economic efficiency maximization control systems." Energy 123 (2017): 585-593.

[32] Foresti.S, Giampaolo.M, and S. Escribano. "Experimental investigation of PEM fuel cells for an m-CHP system with membrane reformer." International Journal of Hydrogen Energy 42.40 (2017): 25334-25350.

[33] Jing, R., Wang, M., Wang, W., Brandon, N., Li, N., Chen, J., & Zhao, Y. (2017). Economic and environmental multi-optimal design and dispatch of solid oxide fuel cell-based CCHP system. *Energy Conversion and Management*, *154*, 365-379.

[34] Moradi, M., & Mehrpooya, M. (2017). Optimal design and economic analysis of a hybrid solid oxide fuel cell and parabolic solar dish collector, combined cooling, heating and power (CCHP) system used for a large commercial tower. *Energy*, *130*, 530-543.

[35] Chahartaghi, M., and B. Alizadeh Kharkeshi. "Performance analysis of a combined cooling, heating and power system with PEM fuel cell as a prime mover." Applied Thermal Engineering 128 (2018): 805-817.

[36] Mehrpooya, M., Sadeghzadeh, M., Rahimi, A., & Pouriman, M. (2019). Technical performance analysis of a combined cooling heating and power (CCHP) system based on solid oxide fuel cell (SOFC) technology–A building application. *Energy Conversion and Management*, *198*, 111767.

[37] You, H., Han, J., & Liu, Y. (2020). Conventional and advanced exergoeconomic assessments of a CCHP and MED system based on solid oxide fuel cell and micro gas turbine. *International Journal of Hydrogen Energy*, *45*(21), 12143-12160.

[38] Zhao, J., Cai, S., Huang, X., Luo, X., & Tu, Z. (2021). 4E analysis and multiobjective optimization of a PEMFC-based CCHP system with dehumidification. *Energy Conversion and Management*, *248*, 114789.

[39] Hou, H., JiwenWu, J., Ding, Z., Yang, B., Hu, E., (2021), Performance analysis of a solar-assisted combined cooling, heating

and power system with an improved operation strategy, Energy, 227, 120516.

[40] Lu, Z., Duan, L., Wang, Z., Zhang, H., (2022), Performance study of solar aided molten carbonate fuel cell-steam turbine-combined cooling, heating and power system with different schemes, Energy Conversion and Management, 263, 115704.

[41] Jaimot, J. (2013). Scope and implementation of standards ASME N510/N511 in air treatment system (HVAC) of the Asco nuclear power plant. In *39 Annual Meeting of Spanish Nuclear Society, September 25-27, 2013, Reus, Tarragona (Spain)*.